JMEPEG (2017) 26:2998–3006
DOI: 10.1007/s11665-017-2724-5

1059-9495/$19.00

Carbon Nanotube-Reinforced Aluminum Matrix Composites Produced by High-Energy Ball Milling

Dilermando N. Travessa, Geovana V.B. da Rocha, Kátia R. Cardoso, and Marcela Lieblich

(Submitted December 2, 2016; in revised form April 24, 2017; published online May 12, 2017)

Although multiwall carbon nanotubes (MWCNT) are promising materials to strengthen lightweight aluminum matrix composites, their dispersion into the metallic matrix is challenge. In the present work, MWCNT were dispersed into age-hardenable AA6061 aluminum alloy by high-energy ball milling and the blend was subsequently hot-extruded. The composite bars obtained were heat-treated by solution heat treatment at 520 °C and artificially aged at 177 °C for 8 h, in order to reach the T6 temper. Special attention was given to the integrity of the MWCNT along the entire composite production. The microstructure of the obtained bars was evaluated by optical and scanning electron microscopy, and the mechanical properties were evaluated by Vickers microhardness tests. Raman spectroscopy, x-ray diffraction and transmission electron microscopy were employed to evaluate the structural integrity of MWCNT. It was found that milling time is critical to reach a proper dispersion of the reinforcing phase. The composite hardness increased up to 67% with the dispersion of 2% in weight of MWCNT, when comparing with un-reinforced bars produced by similar route. However, age hardening was not observed in composite bars after heat treatment. It was also found that MWCNT continuously degraded along the process, being partially converted into Al_4C_3 in the final composite.

Keywords aluminum matrix composite, carbon nanotubes, high-energy ball milling, mechanical properties

1. Introduction

Engineering application of materials, particularly in the competitive automotive, aerospace and energy sectors, demands the design of materials having specific properties. When structural efficiency is concerned, high-strength, low-density materials like Al alloys are highly competitive. Second-phase precipitation is one of the most efficient strengthening mechanisms for aluminum. This efficiency strongly depends on a fine and homogeneous dispersion of a nanoscale hard intermetallic second phase throughout the matrix, obtained by proper alloying combined with optimized thermomechanical processing and heat treatment procedures. The volumetric fraction of the hardening phase depends on the solid solubility limits and seems to be saturated in most of the systems with commercial interest (Ref 1), at least when near-equilibrium thermodynamic based processes are employed.

Carbon nanotubes (CNT) are one of the structural forms of carbon, which exhibit interesting mechanical properties due to its perfect tridimensional (tube) arrangement of sp^2 type carbon covalent bonds. This unique structure results in strength and elastic modulus as high as 50 GPa and 1.8 TPa, respectively, along with a density as small as 1.2 g/cm^3 (Ref 2-4). Such characteristics make CNT very attractive as a reinforcing phase in lightweight metal matrix composites (MMC). It is expected that the presence of nanometric CNT dispersed into a ductile matrix, as aluminum, can promote two distinct hardening mechanisms (Ref 5). The first relates to a direct effect based on the classical load transfer mechanism from the ductile matrix to the strong reinforcing phase, through a tight interface. The second relates to an indirect effect based on the decrease of dislocations mobility due to stress fields in the matrix around the dispersed CNT. In fact, the efficiency of the classical load transfer mechanism in fiber-like reinforcements depends on a minimum length (critical length) (Ref 5), and consequently, the composite processing conditions shall guarantee the CNT integrity. On the other hand, if CNT are fragmented, the Orowan mechanisms can also account for significant hardening (Ref 6). Irrespective to the hardening mechanism, the efficiency depends on a homogeneous dispersion of the reinforcing phase and its proper adhesion to the matrix. If CNT are dispersed into a commercial age-hardenable aluminum alloy, their hardening effect could be added to the strengthening effect of second-phase precipitation obtained by conventional heat treatment. Consequently, the mechanical properties of the resulting composite can increase significantly in comparison with the alloy itself. Recently, an interesting approach to produce microlaminated CNT/high-strength Al alloys has been presented (Ref 7), combining the strengthening effect of aligned CNT with the precipitation hardening of the alloy. In this composite, the resulting structure is lamellar, and CNT are grouped at the inter-lamellar space.

Important contributions in the field of CNT-reinforced MMC and particularly in aluminum matrix composites (AMC) have been published in the last ten years. In these works, the dispersion of the nanometric CNT particles into the

Dilermando N. Travessa, **Geovana V.B. da Rocha**, and **Kátia R. Cardoso**, Instituto de Ciência e Tecnologia – Universidade Federal de São Paulo, ICT-UNIFESP, Rua Talim, 330, São José dos Campos, SP CEP 12231-280, Brazil; and **Marcela Lieblich**, Centro Nacional de Investigaciones Metalurgicas – Consejo Superior de Investigaciones Cientificas, CENIM-CSIC, Avda. Gregorio del Amo, 8, 28040 Madrid, Spain. Contact e-mails: dilermando.travessa@unifesp.br, geovana_dmp@yahoo.com.br, krcardoso@unifesp.br, and marcela@cenim.csic.es.

matrix is always a great concern, as their high surface area results in van der Waals forces that tend to agglomerate them. High-energy ball milling (HEBM) seems to be an efficient method to promote CNT dispersion into aluminum powder. In fact, the great majority of works relating to CNT/AMC production involve at least one step of HEBM. In ductile systems, it is very well known that HEBM develops in stages, starting with particles flattening, cold welding, layering and refracturing. As the CNT dimensions are much smaller than typical Al powers, they can be enveloped by the deformed metal, being protected from direct impact of the milling media. However, it has been demonstrated that longer milling times fragment and amorphize the CNT, making them excessively reactive with aluminum during subsequent high-temperature processing cycles (Ref 8). As the CNT integrity has to be guaranteed in order to them to effectively contribute to the composite strengthening, several works reported attempts to previously disperse the CNT with Al powder in liquid solutions assisted by ultrasonic shaking, in order to reduce subsequent milling time or energy (Ref 9-14). Those attempts were relatively successful, as initial CNT bundles were broken. However, most of CNT remain at grain boundaries in the consolidated composite, contributing mainly with grain refinement rather than with the composite reinforcement. Milling time was demonstrated to be a key issue in order to promote homogeneous dispersion of CNT by HEBM (Ref 15-17), and the matter is to find optimized parameters of time, energy and media that can properly balance an efficient dispersion, minimizing CNT damage.

Most of the works reporting CNT-reinforced AMC are related to pure aluminum and, although significant strengthening has been reported in some cases, the obtained composites only approaches to the mechanical properties of the commercial Al alloys. As already mentioned, very few papers report the use of commercial Al alloys (Ref 7, 9, 10, 18) to produce CNT/AMC. Those alloys are commonly precipitation-hardened, and it seems that there is a very little explored potential to combine two strengthening mechanisms in CNT/AMC: CNT dispersion and precipitation hardening.

In the present work, 1 to 2% (in weight) of multiwall CNT (MWCNT) were dispersed into the age-hardenable commercial AA6061 alloy by high-energy ball milling process (HEBM). The obtained composite powder was consolidated into cylindrical bars by the hot extrusion process. The bars were solution heat-treated and aged, following the best practices recommended to the commercial alloy (Ref 19). The intent was to obtain a material having a strength level higher than the commercial alloy (Ref 20). Raman spectroscopy and x-ray diffraction were performed after each processing step in order to verify the MWCNT integrity. Hardness testing was performed in order to assess the mechanical properties of the resulting composite in the as-extruded condition, as well as after heat treatment. Composite microstructural characterization was performed by optical, scanning and transmission electron microscopy.

2. Experimental Details

AA6061 alloy powder (Alpoco Co., UK) produced by argon gas atomization, with particles lesser than 50 μm, and multiwall carbon nanotubes (MWCNT) Baytubes®C150P (Bayer Materials Science, Germany), produced by chemical vapor deposition, were used in the present work. The MWCNT had a purity level higher than 95%, an average outer diameter of 40 nm and an aspect ratio of about 100. The dispersion of 1-2% in weight of MWCNT in the powder alloy was performed by HEBM process in a Retsch PM4 planetary ball mill (Fritsch, Germany), with a velocity of 200 rpm and a ball-to-powder ratio of 10:1 in air. 0.5% in weight of stearic acid was employed as a process control agent. Hardened steel balls and AISI 304 stainless steel vials were employed. The milling times were 6 and 10 h. Samples containing no MWCNT were also milled for similar time, as a baseline for comparison purpose. Table 1 resumes the different samples obtained. After milling, powder samples were observed by optical microscopy (OM) in an Axio Scope microscope (Zeiss, Germany). Samples were embedded into bakelite, ground in silicon carbide sandpaper and polished in diamond and colloidal silica. For comparison purpose, AA6061 starting powder was also observed, after metallographic etching using Keller's reagent.

The obtained powders were encapsulated into AA6063 tubes (external diameter of 42 mm and wall thickness of 2 mm) and compacted by vibration, up to a density of about 50%. The tube was capped in both ends with AA6063 disks (2 mm thick) and extruded at 450 °C at 2 mm/s, with an extrusion ratio of 28:1. Round bars having 8 mm in diameter and more than 1000 mm long were obtained. The bars' extremities were cut out and discarded, as they contain excess of the caps and tube material. Microstructure and hardness of the bars were evaluated. Optical (Axio Scope Zeiss, Germany) and scanning electron (INSPECT S50 FEI, USA) microscopies were employed for microstructure characterization. Samples were cut and prepared for metallographic examination using similar procedures as described for the powders. Samples were observed at longitudinal and transversal sections, in the as-extruded (AE) and solution heat-treated (T4) conditions. Solution heat treatment was obtained after heating at 520 °C for 1 h, followed by water quenching, and the T4 condition was reached after a 96 h (minimum) of natural aging (room temperature) (Ref 19). In order to obtain the T6 condition, samples in the T4 condition were aged at 177 ± 5 °C for 8 h (Ref 19). Metallographic etching by Keller's reagent was performed in some samples. Transmission electron microscopy, x-ray diffraction and Raman spectroscopy were employed in order to assess the MWCNT integrity during the several steps of the composite processing. Spectra from pristine nanotubes were used as a reference. A micro-Raman microscope system 2000 (Renishaw, UK) operating with an argon laser (514.5 nm wavelength), a 200 kV FEI Tecnai G2 F20 (FEI-USA) transmission electron microscope and an Ultima IV diffractometer (Rigaku, Japan) with Cu Kα radiation (λ = 1,54,178 Å) operating at 40 kV and 30 mA, were employed in these analyses.

Vickers microhardness measurements (TM-7 Future-Tech, Japan) with a load of 1 kg were taken at the cross section of the bars, in the AE, T4 and peak-aged (T6) conditions. Five measurements were taken in each sample, and the average values, along with their respective standard deviation, were recorded.

3. Results and Discussion

Figure 1(a) shows the starting AA6061 powder, observed by optical microscopy after metallographic preparation. It can be observed that particles are predominantly round, exhibiting the

Table 1 Milling conditions employed for MWCNT dispersion into the AA6061 alloy powder

Sample identification	% in weight of MWCNT	Milling time, h
6061 2CNT 6h	2	6
6061 1CNT 6h	1	6
6061 2CNT 10h	2	10
6061 1CNT 10h	1	10
6061 NR 6h	None	6
6061 NR 10h	None	10

typical dendrite structure of the atomized alloy. Particle refining and flattening, typical from ductile particles submitted to HEBM, starts after milling the composite containing 2% of MWCNT for 6 h; see Fig. 1(b). After milling for 10 h, the same powder reaches a complete flattening morphology. The bars obtained after hot extrusion presented a sound aspect, free of defects. A non-recrystallized wrought microstructure was observed after metallographic examination, which is typical for commercial extruded Al alloys. Figure 2 shows the optical micrograph from the sample containing 2% of MWCNT milled for 6 h, in the AE condition. Chemical etching by Keller's reagent did not show any additional detail of the microstructure. Insoluble precipitates (typically Fe_3SiAl_{12}) as well as coarse Mg_2Si precipitates (Ref 21) are visible and aligned with the extrusion direction. This characteristic was common for all bars, irrespective to the addition of MWCNT. These typical precipitates present in commercial AA6061 extruded bars are much finer in the bars produced by HEBM. In the center of Fig. 2, a long and isolated particle is observed. SEM/EDS microanalysis of such particle (not shown here) identified the presence of Fe, Cr and Ni at proportions compatible with the AISI 304 stainless steel. This shows that some contamination from the vials is present in the final bars. It is interesting to note that the extrusion lines contour such particle.

After solution heat treatment, superficial blisters emerged in the bars. These blisters were accompanied by voids observed in the microstructure. Figure 3 shows an optical micrograph of the sample containing 2% of MWCNT milled for 6 h in the T4 condition (after solution heat treatment), where these voids are observed on both longitudinal and transverse sections of the bar (Fig. 3a and b, respectively). These voids are supposed to be related to entrapped air that expands during the solution heat treatment, and are referred as processing defects.

The strength of the obtained composites bars was evaluated by microhardness tests in the AE condition, as well as after heat treatment performed according to the procedures recommended for the commercial alloy (Ref 19) that resulted on T4 and T6 conditions. It is worth mentioning that the hardness measurements were not affected by the voids observed in Fig. 3, as the micro-indentations were obtained on defect-free regions. The results are summarized in Fig. 4. It is possible to observe that MWCNT dispersion by HEBM for 6 h increases the average hardness of the alloy in the AE condition, by about 20 and 32%, as the MWCNT fraction increases from 1 to 2%, respectively (from 72 HV for un-reinforced alloy to 86 and 93 HV for 1 and 2% of MWCNT, respectively). When the HEBM time increases from 6 to 10 h, the increase in the average hardness is even more significant by about 62 and 67% (113 and 121 HV) with the addition of 1 and 2% of nanotubes, respectively. For the un-reinforced bars, the hardness values remain constant, independently of the milling time. The hardness values obtained are very interesting, when comparing with the values of around 76 and 83 HV reported in the literature for 1% in weight CNT-reinforced AA6XX composites (Ref 22, 23). A more expressive result (around 337 HV) has been reported on dual-nanoparticulate (1% in volume SiC and 6% in weight of CNT) reinforced AA6061 matrix composite (Ref 24).

ANOVA and Tukey's test at a confidence level of 5% were performed in order to evaluate the statistical significance of the differences in hardness among the samples. It can be observed from Table 2 that, in fact, there is no statistical difference in adding 1 or 2% of MWCNT or between the un-reinforced bars HEBM for 6 or 10 h. However, the differences are significant when comparing un-reinforced and MWCNT composite bars, as well as composite bars HEBM for 6 or 10 h. These results show that MWCNT indeed strengthen the alloy, and their effects are more significant for higher milling times, where the MWCNT dispersion is supposed to be more homogeneous.

After solution heat treatment and artificial aging (T6 condition), it is observed for all bars that the hardness does not increase, when comparing with the AE condition. The un-reinforced bars showed a decrease in hardness after solution heat treatment (T4 condition) that was counterbalanced after precipitation hardening (T6 condition) reaching the same level as the AE condition. From Fig. 1(a), it can be observed that the starting Al powder presents a typical as-casted structure. During HEBM, this structure can evolve to a supersaturated solid solution (Ref 25). In the present work, it could relate to the dissolution of coarse equilibrium Mg_2Si precipitates into de Al matrix. However, during high-temperature extrusion, reprecipitation of coarse equilibrium precipitates can occur, which does not contribute to the alloy strength. In commercial alloys, the microstructure is optimized by post-extrusion solution/precipitation heat treatment, resulting in hardness increasing from T4 to T6 condition. However, in the present work, it seems that this hardening effect of the precipitation is counterbalanced by softening of the work-hardened microstructure produced by the HEBM/extrusion process. This softening effect is a consequence of recuperation or recrystallization mechanisms.

In the composite bars reinforced by 1% in weight of MWCNT, the hardness slightly increases from T4 to T6 temper, but differently from the un-reinforced bars, the hardness does not reach the value of the AE condition. When 2% in weight of MWCNT is dispersed into the composite, it is observed that hardness seems to continuously decrease through AE-T4-T6 sequence. Softening by recuperation/recrystallization mechanisms seems to occur on both un-reinforced and composite bars. However, subsequent precipitation hardening occurs only partially in the presence of 1% of MWCNT and is suppressed in the presence of 2% of MWCNT. Similar result has been observed by Kondoh and co-workers in AA6063 series alloy reinforced by carbon nanotubes (Ref 23). The authors found that Mg diffused around CNT and was consumed to form Al_2MgC_2 compounds, depleting the matrix of alloying elements and avoiding the formation of the Mg_2Si strengthening phase. Other possibility to explain the deficiency in precipitation hardening of composite bars is that, due to high density of defects introduced by the HEBM process, precipitation kinetics could be changed, and the conventional heat treatment employed to the commercial alloy (Ref 19) is no longer suitable for bars obtained by this route. In such case, peak

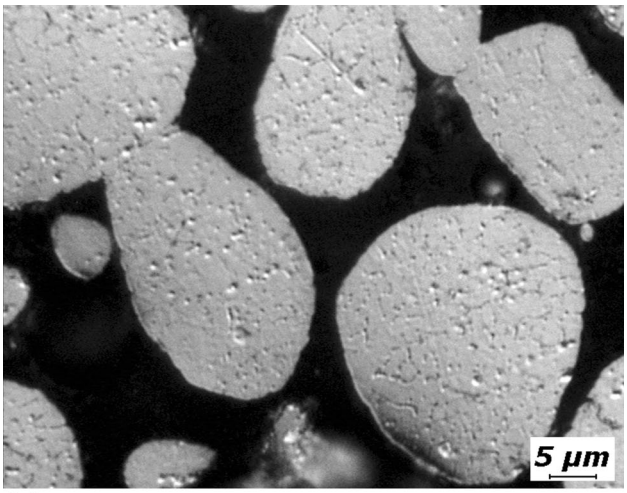

(a)

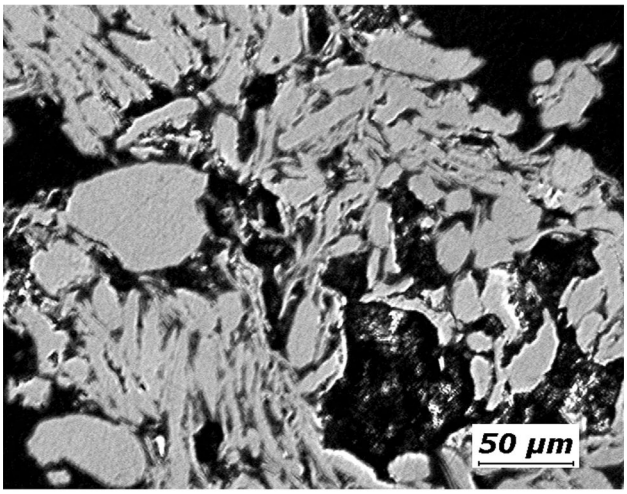

(b)

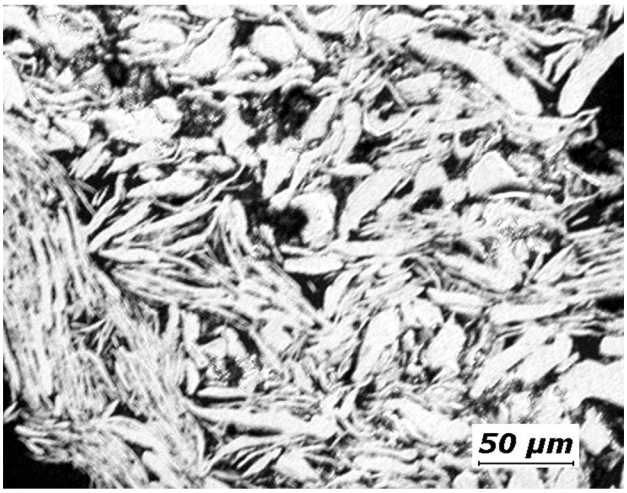

(c)

Fig. 1 (a) Aspect of the AA6061 atomized powder; (b) composite AA6061/MWCNT (2%) powder, after HEBM for 6 h; (c) composite AA6061/MWCNT (2%) powder, after HEBM for 10 h

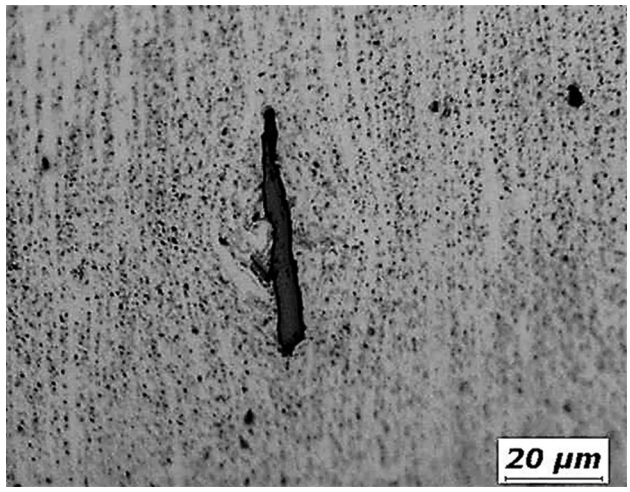

Fig. 2 Optical micrograph of the sample 6061 2CNT 6h, in the as-extruded condition, longitudinal direction

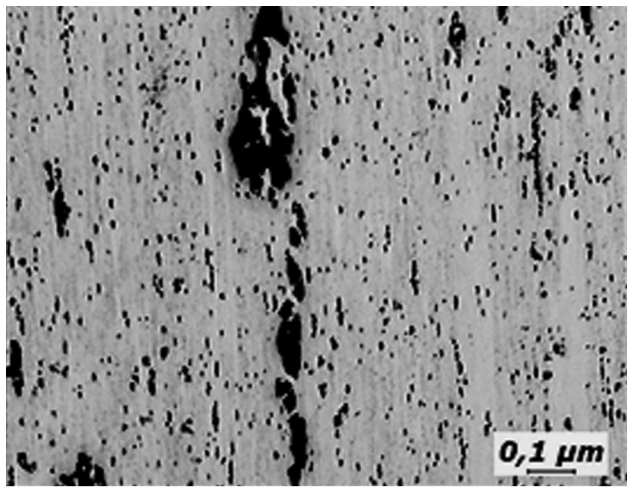

(a)

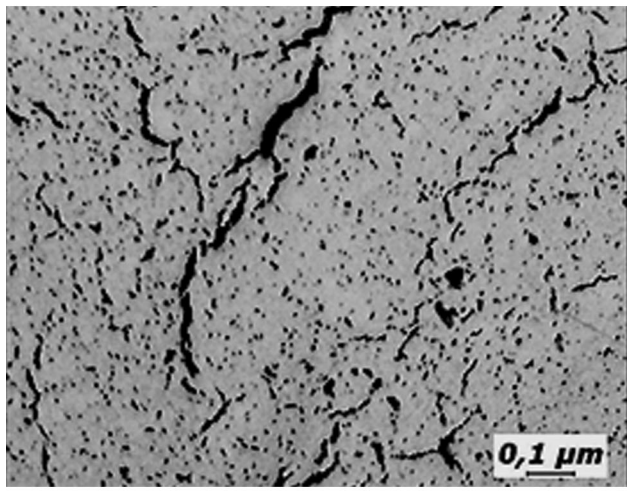

(b)

Fig. 3 Optical micrograph of the sample 6061 2CNT 6h, after solution heat treatment at 520 °C for 1 h (T4 condition): (a) longitudinal and (b) cross sections

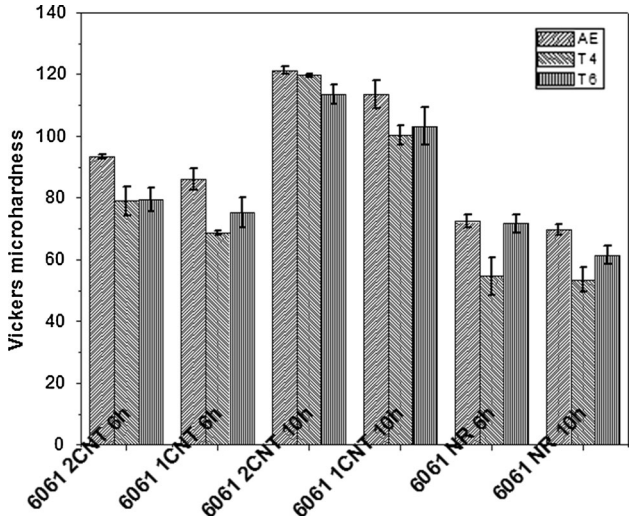

Fig. 4 Vickers microhardness values obtained for the extruded bars, in the as-extruded, T4 and T6 conditions

Table 2 Tukey's test (5% probability level) performed on hardness test results

Sample	AE	T4	T6
6061 2CNT 6h	a	d	h
6062 1CNT 6h	a	d	h,i
6061 SR 6h	b	e	h,i
6061 2CNT 10h	c	f	j
6062 1CNT 10h	c	g	j
6061 SR 10h	b	e	i

Inside the column, the same letter indicates that the results are statistically equal

hardening could be reached at shorter aging times. Finally, a third possibility to explain the inefficiency of heat treatment in the composite bars would be a grain refinement produced by HEMB in the presence of the nanotubes. This effect has been observed (Ref 26), and the resulting higher grain boundary area can promote coarse precipitation at grain boundaries instead of fine precipitation inside the grains (Ref 27). The solute-depleted zones, also called precipitation-free zones, are commonly observed in commercial aluminum alloys. However, their effect is less significant in microsized grain than in nanosized grain alloys.

ANOVA and Tukey's test performed in hardness results from samples at T4 and T6 conditions reveal that the addition of MWCNT indeed contributes to the alloy strength, as already mentioned, when the milling time was 10 h. This shows that the milling time is critical to produce high-strength composites, due to a better dispersion of the nanotubes that increases their strengthening efficiency. However, it seems that the structure of the MWCNT is increasingly degraded, after each step of the composite production. Figure 5 shows the Raman spectroscopy of the composites in the as-milled powder and in the bars on both as-extruded (AE) and solution heat-treated (T4) conditions. The presence of first- and second-orders D, G and G' bands in all conditions can be observed, around their typical values for the incident laser energy employed: 1350, 1580 and 2684 cm^{-1}, respectively. D + G band around 2920 cm^{-1} is

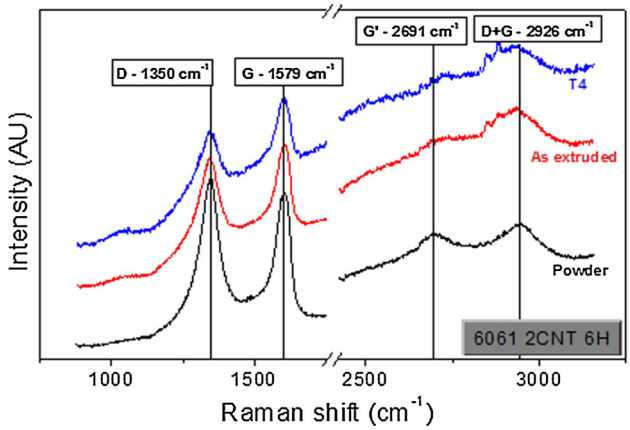

Fig. 5 Raman spectroscopy of the composite containing 2% of MWCNT, prepared after 6 h of HEBM

also present in all samples. However, as the composite is exposed to the high-temperature cycles of extrusion and solution heat treatment, the peaks become less intense, and particularly, the G' band seems to disappear. As the G band and its second-order scatter G' are frequently related to the structural order of carbon-based materials (Ref 28, 29), it seems that during the high-temperature processing cycles, the structure of the MWCNT becomes more imperfect.

In order to check the presence of hardening precipitates in the bars, TEM analysis was performed. Figure 6 shows the aspect of the un-reinforced bar produced by HEBM for 6 h, in the as-extruded condition. A fine grain structure can be observed, with some of the grains exhibiting high density of dislocations (Fig. 6a). Higher magnification (Fig. 6b) reveals the presence of round-shaped precipitates in the order of 100 nm, along with a very thin un-identified homogeneously dispersed precipitates into the grains. EDS microanalysis (Fig. 6c) performed on the bigger round-shaped precipitates reveals the presence of Al-Fe-Si atoms, suggesting the typical insoluble inclusions present in commercial alloys (Ref 30). Figure 7 shows the same bar, after solution heat treatment and aging (T6 condition). When comparing Fig. 7(a) with Fig. 6(a), the presence of the same insoluble inclusions is observed; however, it seems that the dislocation density is higher in the AE condition, which could explain the partial softening observed after solution heat treatment. In Fig. 7(b), an intense fine needle-like precipitation is observed to form after T6 aging, which is compatible with the metastable β'' Mg_2Si phase (Ref 30-32). Based on these observations, it can be concluded that the heat treatment performed in the un-reinforced bar has been satisfactory in obtaining the precipitation hardening effect, agreeing with the hardness increase observed when aging from T4 to T6 condition.

Figure 8 shows the microstructure of the bar containing 2% of MWCNT, in the AE condition. In 8A, when comparing Fig. 6(a) and 7(a), the grains are much thinner and more equiaxed. In 8B, the formation of an un-identified phase around some of the grain boundaries is observed. It would be expected that MWCNT could accumulate into the grain boundaries of the matrix, but the morphology of the observed phase does not match with the nanotubes morphology. One could expect that reaction of nanotubes with the aluminum matrix, as observed by some authors (Ref 8, 33-35), could produce the Al_4C_3 phase

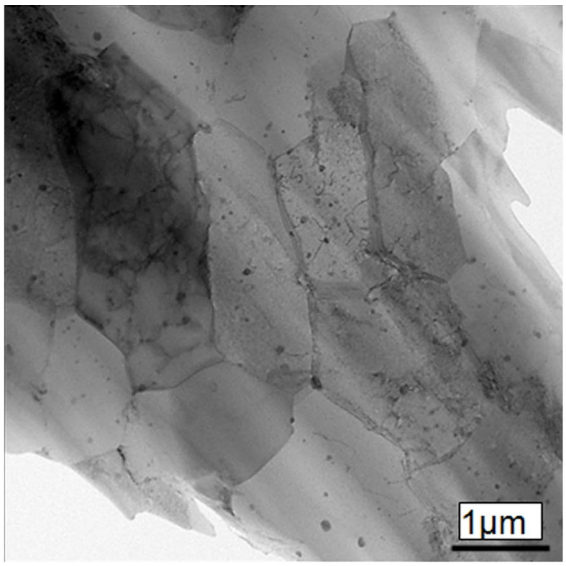

(a)

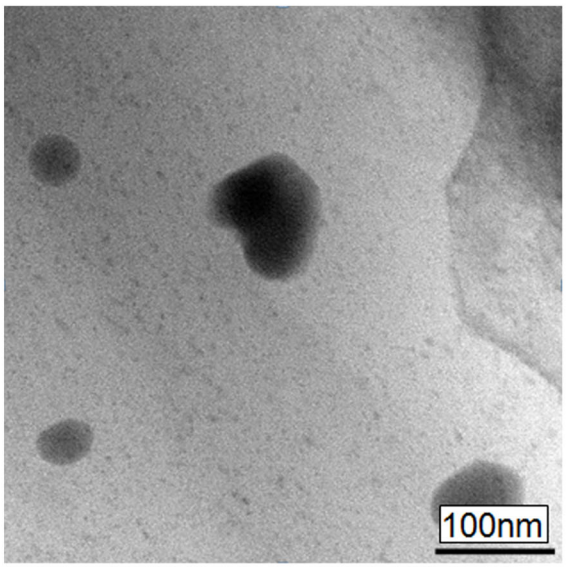

(b)

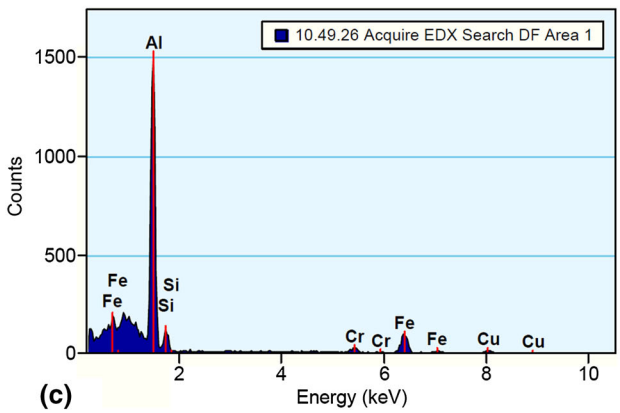

(c)

Fig. 6 TEM images obtained for the un-reinforced bar produced by HEBM for 6 h, in the AE condition. In C the EDS microanalysis result from the round-shaped precipitates seen in B

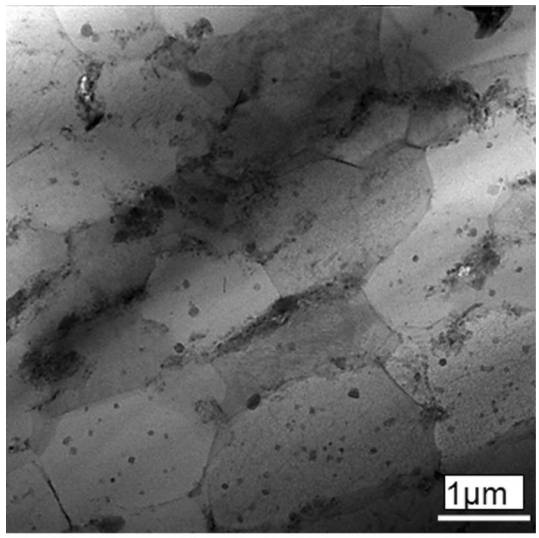

(a)

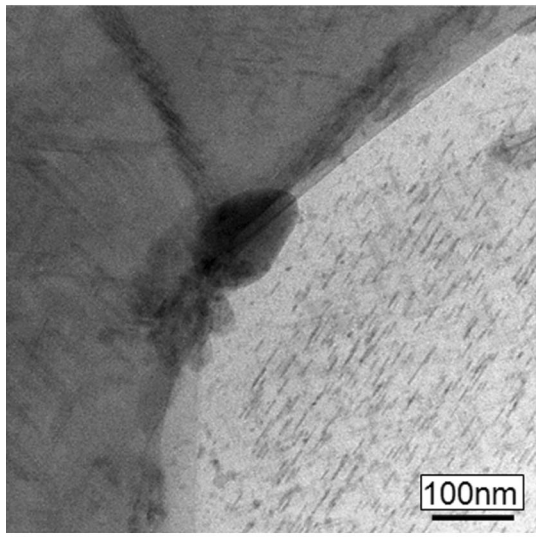

(b)

Fig. 7 TEM images obtained for the un-reinforced bar produced by HEBM for 6 h, after solution heat treatment and aging for 177 °C for 8 h (T6 condition)

at the composite grain boundaries. X-ray diffraction analysis was performed on un-reinforced and 2% reinforced composite bars in both AE and T6 conditions, HEBM for 10 h. The results are shown in Fig. 9. The Y axis is expanded in order to show the low-intensity peaks. It can be observed that peaks of Mg_2Si are present in all samples, being more intense in the AE condition. On the other hand, peaks of the phase Al_4C_3 are present on the samples containing MWCNT, being more intense in T6 condition. These results suggests that, during high-temperature production cycles like hot extrusion and mainly solution heat treatment, nanotubes present at grain boundaries have reacted in some extension with the matrix, producing aluminum carbide. It has also to be pointed out that the carbon (002) diffraction peak at $2\theta = 26°$, expected due to the presence of carbon nanotubes, was not observed in the XRD patterns, probably due to their small amount. Further-

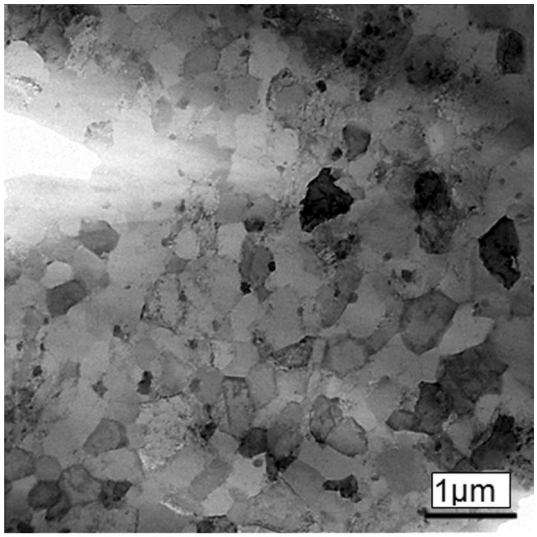

(a)

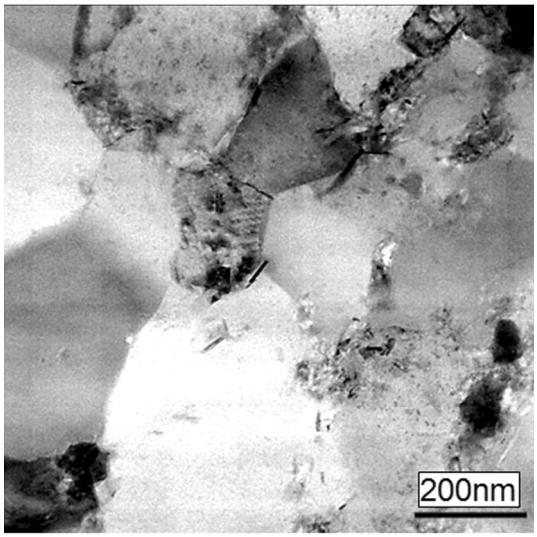

(b)

Fig. 8 TEM images obtained for the 2% MWCNT composite bar produced by HEBM for 10 h, in the AE condition

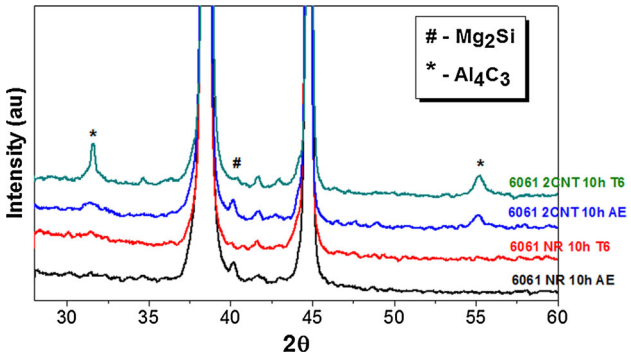

Fig. 9 Results from x-ray diffraction of un-reinforced and 2% of MWCNT composite bars, produced using powders milled for 10 h. These bars were analyzed on both AE and T6 conditions. The high-intensity peaks correspond to Al

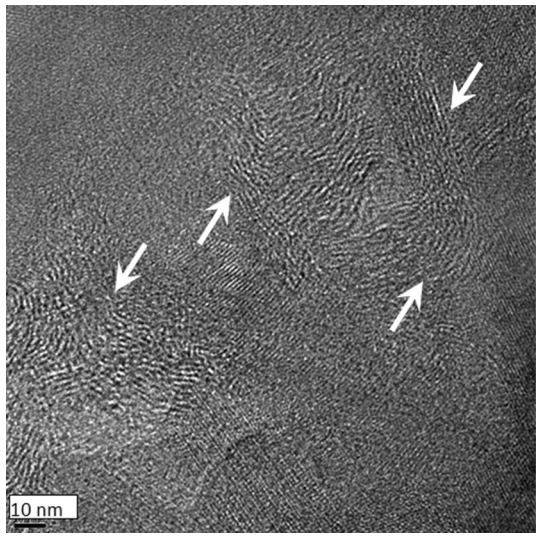

Fig. 10 HRTEM image obtained for the 2% MWCNT composite bar produced by HEBM for 10 h, in the T6 condition

more, some alloying elements can also accumulate at these regions, reducing the formation of the Mg_2Si hardening phase.

HRTEM image obtained from the 2% MWCNT composite bar HEBM for 10 h, in the T6 condition, is shown in Fig. 10. The waved morphology regions marked by arrows in the figure strongly suggest that some MWCNT could be intact in the interior of the grains. It can also be observed that the interface between these supposed nanotubes and the matrix is tight and no intermediate compounds seem to be formed. From these results, it can be inferred that MWCNT which were enveloped by Al alloy powder during initial stages of HEBM were protected from the severity of the process, keeping their structural integrity and stability during the overall processing cycle of the composite. On the other hand, unprotected MWCNT that accumulate around the alloy powder were damaged, reacting with Al and alloying elements during the subsequent composite processing. TEM images of the same bar containing 2% of MWCNT and HEBM for 10 h are shown in Fig. 11. In 11A, it can be observed that some grains seem to grow after solution heat treatment and aging, when compared to Fig. 8(a). In 11B, some coarse needle-shaped precipitates about 50 to 100 nm long are observed, which could be compatible with the β' Mg_2Si metastable precipitates that have poor contribution to the alloy hardening (Ref 30, 31). The very fine precipitation of the β'' Mg_2Si was not observed in this sample, suggesting, as observed from the hardness tests, that the MWCNT-reinforced alloy was not peak age-hardened when performing heat treatment according to the recommended practices for the commercial alloy.

4. Conclusions

Based on the results obtained in the present work, the following conclusions can be drawn:

– MWCNT-reinforced AA6061 aluminum matrix composites have been successfully produced by HEBM followed by consolidation using the hot extrusion process. The obtained

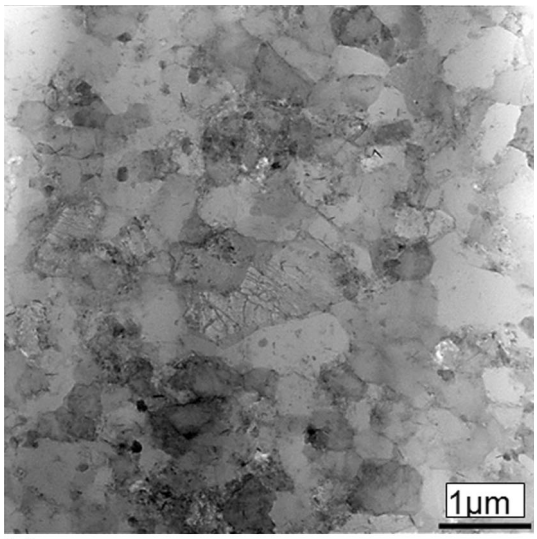

(a)

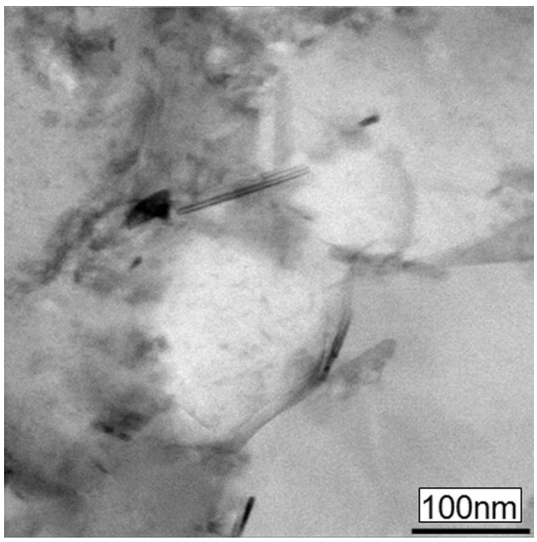

(b)

Fig. 11 TEM images obtained for the 2% MWCNT composite bar produced by HEBM for 6 h, after solution heat treatment and aging for 177 °C for 8 h (T6 condition)

bars showed a typical un-recrystallized wrought microstructure.

- Raman spectroscopy reveals some disorder increase on the MWCNT structure, as the composite production proceeds. This disorder seems to be enhanced after the cycles involving temperature. G' band, still present in the as-milled powder, significantly decreases after hot extrusion. After solution heat treatment, G' band practically disappeared.
- The hardness of the composite bars increased by about 20% when 1% in weight of MWCNT was incorporated to the alloy, when compared to a bar produced by the same processing route, with no nanotubes addition. When adding 2% of MWCNT, the hardness increased by about 32%. Increasing the HEBM time from 6 to 10 h, for 2% of MWCNT addition, the hardness increased by about 67%. This result seems to be related to better nanotubes dispersion, as the milling time increases.
- Solution heat treatment and precipitation aging procedures, typical for commercial AA6061 extruded bars, did not result in increase of the hardness, when compared to the AE condition. For the un-reinforced bar, hardness in T6 condition increased related to the T4, but reached the same level as the AE condition. In this case, it is believed that precipitation hardening was counterbalanced by the microstructure softening. In the presence of the MWCNT, the hardness of the composite bars in T6 condition did not even reach the AE level. In this case, it seems that the precipitation phenomenon has been somehow suppressed in the presence of the nanotubes and due to HEBM.
- TEM analysis showed that, in the presence of MWCNT, the microstructure is finer. However, there are indications of degraded nanotubes at grain boundaries that apparently form Al carbides, as indicated by the x-ray diffraction results. On the other hand, there are indications by HRTEM that some of MWCNT, enveloped by the ductile alloy particles during the initial stages of HEBM, remain unchanged in the interior of the composite grains. Differently from the un-reinforced bars, β" Mg_2 Si hardening phase precipitation was not observed in composite bars after heat treatment to T6 condition.

Acknowledgments

The authors are thankful to the Associated Laboratory for Sensors and Materials (LAS-INPE-Brazil), for the Raman Spectroscopy analysis, and to FAPESP for the financial support (Process Nos. 2012/07831-2 and 2013/10570-9).

References

1. J. Liu and M. Kulak, A New Paradigm in the Design of Aluminum Alloy for Aerospace Application, *Mater. Sci. Forum*, 2000, **331–337**, p 127–140
2. E.T. Thostensona, Z. Renb, and T.W. Choua, Advances in the Science and Technology of Carbon Nanotubes and Their Composites: A Review, *Compos. Sci. Technol.*, 2001, **61**, p 1899–1912
3. M. Paradise and T. Goswami, Carbon Nanotubes—Production and Industrial Applications, *Mater. Des.*, 2007, **28**, p 1477–1489
4. R. George, K.T. Kashyap, R. Rahul, and S. Yamdagni, Strengthening in Carbon Nanotube/Aluminium (CNT/Al) Composites, *Scr. Mater.*, 2005, **53**, p 1159–1163
5. H.J. Choi, J.H. Shin, and D.H. Bae, Grain Size Effect on the Strengthening Behavior of Aluminum-Based Composites Containing Multi-walled Carbon Nanotubes, *Compos. Sci. Technol.*, 2011, **71**, p 1699–1705
6. W.S. Miller and F.J. Humphreys, Strengthening Mechanisms in Particulate Metal Matrix Composites, *Scr. Metall. Mater.*, 1991, **25**, p 33–38
7. H. Wei, Z. Li, D.-B. Xiong, Z. Tan, G. Fan, Z. Qin, and D. Zhang, Towards Strong and Stiff Carbon Nanotube-Reinforced High-Strength Aluminum Alloy Composites Through a Microlaminated Architecture Design, *Scr. Mater.*, 2014, **75**, p 30–33
8. D. Poirier, R. Gauvin, and A.L.D. Robin, Structural Characterization of a Mechanically Milled Carbon Nanotube/Aluminum Mixture, *Compos. A*, 2009, **40**, p 1482–1489
9. C. Deng, D. Wang, X.X. Zhang, and A.B. Li, Processing and Properties of Carbon Nanotubes Reinforced Aluminum Composites, *Mater. Sci. Eng. A*, 2007, **444**, p 138–145
10. C. Deng, X.X. Zhang, D. Wang, Q. Lin, and A.B. Li, Preparation and Characterization of Carbon Nanotubes/Aluminum Matrix Composites, *Mater. Lett.*, 2007, **61**, p 1725–1728

11. A.M.K. Esawi and M.A. El Borady, Carbon Nanotube-Reinforced Aluminium Strips, *Compos. Sci. Technol.*, 2008, **68**, p 486–492
12. K. Morsi, A.M.K. Esawi, S. Lanka, A. Sayed, and M. Taher, Spark Plasma Extrusion (SPE) of Ball-Milled Aluminum and Carbon Nanotube Reinforced Aluminum Composite Powders, *Compos. A*, 2010, **41**, p 322–326
13. A.M.K. Esawi, K. Morsi, A. Sayed, M. Taher, and S. Lanka, Effect of Carbon Nanotube (CNT) Content on the Mechanical Properties of CNT Reinforced Aluminium Composites, *Compos. Sci. Technol.*, 2010, **70**, p 2237–2241
14. D.N. Travessa and M. Lieblich, Dispersion of Carbon Nanotubes in AA6061 Aluminium Alloy Powder by the High Energy Ball Milling Process, *Mater. Sci. Forum*, 2014, **802**, p 90–95
15. A.M.K. Esawi and K. Morsi, Dispersion of Carbon Nanotubes (CNTs) in Aluminum Powder, *Compos. A*, 2007, **38**, p 646–650
16. L. Wang, H. Choi, J. Myoung, and W. Lee, Mechanical Alloying of Multi-walled Carbon Nanotubes and Aluminium Powders for the Preparation of Carbon/Metal Composites, *Carbon*, 2009, **47**, p 3427–3433
17. A.M.K. Esawi, K. Morsi, A. Sayed, A.A. Gawad, and P. Borah, Fabrication and Properties of Dispersed Carbon Nanotube-Aluminum Composites, *Mater. Sci. Eng. A*, 2009, **508**, p 167–173
18. C.F. Deng, X.X. Zhang, D.Z. Wang, and Y.X. Ma, Calorimetric Study of Carbon Nanotubes and Aluminum, *Mater. Lett.*, 2007, **61**, p 3221–3223
19. Aerospace Material Specification. Society of Automobile Engineers—SAE AMS2772E: *Heat Treatment of Aluminum Alloy Raw Materials*. SAE International, 2008
20. Aerospace Material Specification. Society of Automobile Engineers—SAE. AMS-QQ-A-200/8: *Aluminum Alloy 6061, Bar, Rod, Shapes, Tube, and Wire, Extruded*. SAE International, 2007
21. D.S. MacKenzie and G.E. Totten, *Analytical characterization of aluminium, steel, and superalloys*, CRC Press—Taylor & Francis Group, Boca Raton, 2006
22. Y. Wu, G.-Y. Kim, and A.M. Russell, Effects of Mechanical Alloying on an Al6061–CNT Composite Fabricated by Semi-solid Powder Processing, *Mater. Sci. Eng. A*, 2012, **538**, p 164–172
23. K. Kondoh, H. Fukuda, J. Umeda, H. Imai, and B. Fugetsu, Microstructural and Mechanical Behavior of MWCNTs Reinforced Al-Mg-Si Alloy Composites in Aging Treatment, *Carbon*, 2014, **72**, p 15–21
24. H. Kwon, M. Saarna, S. Yoon, A. Weidenkaff, and M. Leparoux, Effect of Milling Time on Dual-Nanoparticulate-Reinforced Aluminum Alloy Matrix Composite Materials, *Mater. Sci. Eng. A*, 2014, **590**, p 338–345
25. C. Suryanarayana, Mechanical Alloying and Milling, *Prog. Mater. Sci.*, 2001, **46**, p 1–184
26. H. Zare, M. Jahedi, M.R. Toroghinejad, M. Meratian, and M. Knezevic, Microstructure and Mechanical Properties of Carbon Nanotubes Reinforced Aluminum Matrix Composites Synthesized Via Equal-Channel Angular Pressing, *Mater. Sci. Eng. A*, 2016, **670**, p 205–216
27. J. Corrochano, M. Lieblich, and J. Ibáñez, On the Role of Matrix Grain Size and Particulate Reinforcement on the Hardness of Powder Metallurgy Al-Mg-Si/$MoSi_2$ Composites, *Compos. Sci. Technol.*, 2009, **69**, p 1818–1824
28. M.S. Dresselhaus, G. Dresselhaus, R. Saito, and A. Jorio, Raman Spectroscopy of Carbon Nanotubes, *Phys. Rep.*, 2005, **409**(2), p 47–99
29. E.F. Antunes, A.O. Lobo, E.J. Corat, V.J. Trava-Airoldi, A.A. Martin, and C. Veríssimo, Comparative Study of First-and Second-Order Raman Spectra of MWCNT at Visible and Infrared Laser Excitation, *Carbon*, 2006, **44**(11), p 2202–2211
30. I. Dutta and S.M. Allen, A Calorimetric Study of Precipitation in Commercial Aluminium Alloy 6061, *J. Mater. Sci. Lett.*, 1991, **10**, p 323–326
31. G.A. Edwards, K. Stiller, G.L. Dunlop, and M.J. Couper, The Precipitation Sequence in Al-Mg-Si Alloys, *Acta Mater.*, 1998, **46**, p 3893–3904
32. D. Maisonnette, D.M. Suery, D. Nelias, P. Chaudet, and T. Epicier, Effects of Heat Treatments on the Microstructure and Mechanical Properties of a 6061 Aluminium Alloy, *Mater. Sci. Eng. A*, 2011, **528**, p 2718–2724
33. B. Boesl, D. Lahiri, S. Behdad, and A. Agarwal, Direct Observation of Carbon Nanotube Induced Strengthening in Aluminum Composite Via in situ Tensile Tests, *Carbon*, 2014, **69**, p 79–85
34. H. Kwon, M. Estili, K. Takagi, T. Miyazaki, and A. Kawasaki, Combination of Hot Extrusion and Spark Plasma Sintering for Producing Carbon Nanotube Reinforced Aluminum Matrix Composites, *Carbon*, 2009, **47**, p 570–577
35. L. Ci, Z. Ryu, N.Y. Jin-Phillipp, and M. Ruhle, Investigation of the Interfacial Reaction Between Multi-walled Carbon Nanotubes and Aluminum, *Acta Mater.*, 2006, **54**, p 5367–5375